International Journal of Hydrogen Energy 170 (2025) 150996

Contents lists available at ScienceDirect

International Journal of Hydrogen Energy

journal homepage: www.elsevier.com/locate/he

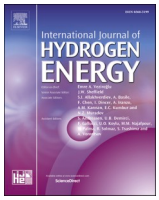

Energy-saving and carbon reduction potential of coal-water slurry gasification: A coupled material and energy flow analysis

Chao Linghu [a,b], Binxuan Zhou [b], Xingxing Cheng [b,c,*], Jiansheng Zhang [b,d], Wenlong Mo [e,f]

[a] College of Chemistry and Chemical Engineering, Taiyuan University of Technology, Taiyuan, 030024, Shanxi, China
[b] Shanxi Research Institute of Huairou Laboratory, Taiyuan, 030032, Shanxi, China
[c] School of Energy and Power Engineering, Shandong University, Jinan, 250061, Shandong, China
[d] Shanxi Clean Energy Research Institute of Tsinghua University, Taiyuan, 030032, Shanxi, China
[e] State Key Laboratory of Chemistry and Utilization of Carbon Based Energy Resources and Key Laboratory of Coal Clean Conversion & Chemical Engineering Process (Xinjiang Uyghur Autonomous Region), College of Chemical Engineering and Technology, Xinjiang University, Urumqi, 830017, Xinjiang, China
[f] Xinjiang Yihua Chemical Industry Co., Ltd., Changji, 831700, Xinjiang, China

ARTICLE INFO

Keywords:
Gasification
Simulation modeling
Energy conservation potential
Exergy loss
Carbon emission

ABSTRACT

This study simulates and models the coal-water slurry gasification using Aspen plus, verifies the accuracy and reliability of the model through actual factory data. Furthermore, combined with the analysis of material-energy flow, the material transformation and energy changes throughout the process are quantified. The results show that the exergy loss of the system accounts for 33.18 % of the total exergy, mainly concentrated in the excitation cooling unit, gasification unit and flash evaporation unit. The exergy losses account for 66.73 %, 27.57 % and 14.58 % of the total exergy loss respectively. The main carbon emission sources are the gasification unit and the flash evaporation unit, with their carbon emissions accounting for 74.98 % and 20.62 % of the total emissions respectively. Finally, forward the targeted optimization suggestion. This research provides a feasible solution for energy conservation and carbon reduction of technology, providing reference value for the low-carbon development of industry.

1. Introduction

Affected by population and economic growth, the demand for energy in countries around the world will continue to increase [1],to cope with the pressure brought about by the scarcity of domestic resources and the slowdown of economic growth. Meanwhile, geopolitical political crises has led fossil fuel suppliers to reduce their supply [2],the rapid industrialization of industrialized countries has also accelerated their own energy consumption [3,4]. Excessive energy consumption, extremely unbalanced energy distribution and the problem of global resource scarcity have led to serious energy security crises for all countries [5]. Meanwhile, the consumption of fossil fuels has significantly exacerbated environmental degradation and ecological damage [6–8]. The growth model centered on fossil energy poses a threat to the sustainable development of the countries in the Comprehensive Economic Partnership (RCEP) [9]. Bashir studied the asymmetric relationship between environmental degradation and related factors using methods such as CS-ARDL [10],confirmed that the consumption of fossil energy has increased environmental pollutants. Xu also adopted the above-mentioned method and confirmed that the environmental Kuznets curve (EKC) hypothesis holds true [3],indicated the adverse impact of the consumption of fossil fuels on the ecological environment. Therefore, replacing traditional fossil fuels with clean energy [11], or optimizing fuel usage methods [12,13], has received considerable attention.

Coal is one of the main fossil energy sources causing air pollution [14], the clean and efficient utilization of coal has become a key concern for countries around the world [15],Clean coal technology (CCT) has developed rapidly [16]. Among them, coal gasification technology is one of the core technologies [16]. It can convert coal into cleaner syngas [17], and reduce the emission of pollutants while improving energy utilization efficiency [17]. However, affected by the process characteristics, there are significant energy losses in each link of the coal gasification process [18,19],resulting in a relatively low overall energy

* Corresponding author. Shanxi Research Institute of Huairou Laboratory, Taiyuan, 030032, Shanxi, China.
E-mail addresses: 2024310166@link.tyut.edu.cn (C. Linghu), zbx_4023@163.com (B. Zhou), xcheng@sdu.edu.cn (X. Cheng), zhang-jsh@tsinghua.edu.cn (J. Zhang), mowenlong@xju.edu.cn (W. Mo).

https://doi.org/10.1016/j.ijhydene.2025.150996
Received 18 June 2025; Received in revised form 11 August 2025; Accepted 13 August 2025

efficiency, and the product contains a certain amount of CO_2 [20]. Furthermore, the carbon in the system does not react completely, reducing the carbon conversion rate [21] and affecting the yield of syngas. Under the constraints of the "dual carbon" goals [22],how to reduce energy consumption through systematic energy-saving optimization [8] and reduce carbon emissions [8,23],has become a key challenge for the sustainable development of this technology.

Experimental research often consumes many resources and time, increasing costs. Compared with experimental research, simulation calculation shows greater advantages. In recent years, various models have been used for the simulation of actual complex working conditions [24–26]. People have carried out simulation calculations [27,28] of related processes by means of Computational Fluid Dynamics (CFD), artificial neural networks (ANN) [29], and thermodynamic equilibrium [30–32], etc. Alobaid simulated multiphase flow, particle interaction and transfer processes in fluidized beds through CFD, evaluated the applicability of different numerical models (such as two-fluid models, soft sphere/hard sphere models), and verified the key role of CFD in the optimization of fluidized bed systems [33]. Tang achieved precise prediction of the three-dimensional NOx concentration distribution in power plants by fusing CFD simulation with DCS operation data, combining the K-means algorithm and the theory-guided deep neural network (TG-DNN), providing an effective monitoring means for low-emission and efficient operation [34]. Naqvi systematically studied the co-pyrolysis process of rice husks, sewage sludge and their mixtures through thermogravimetric analysis combined with kinetic models and artificial neural networks (ANN). It was found that the diffusion model had the best fitting effect in the temperature range of 200–600 °C (R^2 = 0.99), and the efficient resource recovery potential of the co-pyrolysis technology was verified through thermodynamic parameters and ANN [35]. Among them, the Aspen Plus software performs outstandingly in the simulation of the actual coal gasification process. Furthermore, energy-saving potential Analysis, especially Material Flow Analysis (MFA) and Exergy analysis, plays an important role in the process of process optimization [36,37]. MFA can precisely track the transformation and loss paths of raw materials [38],reveal the utilization efficiency of elements such as carbon and hydrogen during the gasification process [39]. Exergy analysis is based on the second law of thermodynamics and reflects the energy grade of each unit in the process [40], display the energy flow of the system and the energy transformation between units [18]. The coupling analysis of the two is crucial for the improvement of the coal-water slurry gasification and the enhancement of system energy efficiency. However, there are few studies on the coupled analysis of material flow and energy flow for this complete process.

In this study, the model of coal-water slurry gasification was constructed using Aspen plus software. Through the sensitivity analysis tool built into the model, the influence of O_2 and steam input amounts on various parameters of the system was studied. For the first time, the method of coupled analysis of material flow and energy flow was adopted, combined with software simulation, to systematically investigate the energy-saving and carbon reduction potential of the process, aiming to provide a scientific basis for the efficient and low-carbon operation of coal-water slurry gasification.

2. Process modeling and methods

2.1. Technological process

The coal-water slurry gasification can be summarized into four main treatment units: the coal-water slurry preparation unit, the coal gasification unit, the syngas washing unit and the black water flash evaporation unit. To facilitate the subsequent research, the complex technological process was simplified. The simplified technological process is shown in Fig. 1.

Coal-water slurry is pumped into the gasifier by a high-pressure coal slurry pump, then reacts with O_2 and steam inside the gasifier. Under high temperature and high-pressure conditions, the reaction is rapidly completed and generates crude synthesis gas, high-temperature molten slag and other substances. The main reactions are as follows:

$$C + 0.5O_2 \rightarrow CO - 110.4kJ/mol \quad (1)$$

$$C + O_2 \rightarrow CO_2 - 393.8kJ/mol \quad (2)$$

$$C + H_2O \rightarrow CO + H_2 + 135.0kJ/mol \quad (3)$$

$$C + 2H_2 \rightarrow CH_4 - 84.3kJ/mol \quad (4)$$

$$C + CO_2 \rightarrow 2CO + 173.3kJ/mol \quad (5)$$

$$CO + H_2O \rightarrow H_2 + CO_2 - 38.4kJ/mol \quad (6)$$

$$CO + 0.5O_2 \rightarrow 2CO_2 - 282.9kJ/mol \quad (7)$$

$$H_2 + 0.5O_2 \rightarrow H_2O - 241.8kJ/mol \quad (8)$$

The product flows downward into the cooling chamber and its temperature drops sharply to 200–300 °C after being cooled by the cooling water. The crude syngas enters the washing unit, is washed in the washing tower and then goes to the subsequent shift and flare system. The washing grey water is sent to the black water flash evaporation unit for further treatment. The black water produced in the excitation cooling unit is sent to the flash evaporation unit and undergoes flash treatment through three-stage flash evaporation system. The three-stage flash evaporation process achieves heat energy recovery from the black water through a series of pressure reductions. Different operating pressures are utilized to gradually concentrate on the black water, thereby

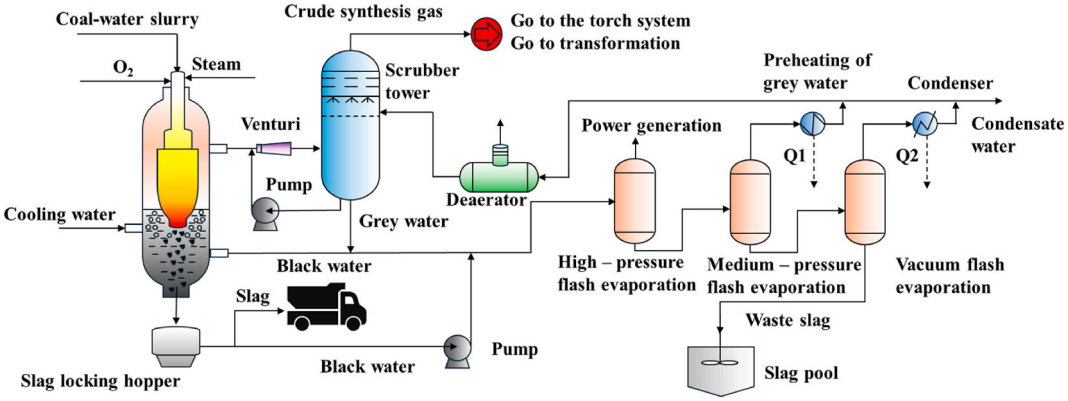

Fig. 1. Technological process of the coal-water slurry gasification.

reducing its volume and achieving its resource utilization. Solid slag after rapid cooling is discharged through the slag locking hopper and sent to the slag pool.

2.2. Simulation modeling of the process

With the help of the rich processing units in the Aspen plus software database, the model of the above-mentioned process flow was constructed, as shown in Fig. 2. The main operation units and their uses in the model are shown in Table 1. Firstly, the physical properties of each component involved in the system are defined. Among them, coal and ash are non-pure substances and are defined as unconventional components. According to the empirical correlation formula, the enthalpy and density are defined and calculated using the HCOALGEN and DCOALIGT models. Coal gasification involves high temperature, high pressure and complex multiphase reactions. Therefore, PR-BM using the Boston-Mathias temperature function α (T) is adopted as the physical property method to improve the simulation accuracy and the calculation accuracy of the thermodynamic behavior of coal. Then, to improve the convergence of the model, the appropriate module is selected to simulate each processing unit in the process. Coal first undergoes pyrolysis, which is completed in the RYield reactor and converted into C (CISOLID), H_2, O_2, S (CISOLID), N_2 and ash (inert) that can enter the subsequent stream. The yields of the above components are correlated and calculated through the FORTRAN subroutine of the software. Set up a component separator (SEP1) to separate the incompletely reacted carbon. The gasification reaction is accomplished by an R-Gibbs reactor, which limits the chemical equilibrium through specified reactions to minimize the Gibbs free energy of the system. The gasification products and residual carbon are mixed through the mixer (H1). The mixed flow streams complete the rapid cooling process through heat exchangers (COOL-1, COOL-2). The crude syngas is washed and separated by SEP4, and the remaining substances such as grey water enter the subsequent treatment unit. Black water and grey water are treated through FLASH generators.

2.3. Assumptions

To simplify the process, highlight the main modules and operation units specifically, and improve the simulation calculation rate, the following assumptions are made in this study.

- All research processes are based on dynamic equilibrium.
- The generation of tar and phenolic substances during the coal pyrolysis process is not taken into account.
- The ash in coal is an inert component and does not participate in the reaction.

Table 1
Each module of the simulation model and its purpose.

Name	Meaning	Unit purpose
RYIELD	Yield reactor	Convert coal into C, H, S, O, N and other substances
RGIBBS	Gibbs reactor	Main body of Gasification reaction
SEP1	Component Separator 1	Separate residual carbon
H1	Mixer 1	Mixed residual carbon and products
SEP2	Component Separator 2	Separate the gas and solid phases
COOL-1	Heat Exchanger 1	Adjust the temperature (gas quenching)
COOL-2	Heat Exchanger 2	Adjust the temperature (solid quenching)
SEP3	Component Separator 3	Separate solid and liquid phases
SEP4	Component Separator 4	Gas washing, separating gas and solid
FLASH1	Flash evaporation 1	High-pressure flash evaporation
COOL-3	Heat Exchanger 3	Reduce the temperature of the ash
FLASH2	Flash evaporation 2	Medium-pressure flash evaporation
COOL-4	Heat Exchanger 4	Condensing steam
FLASH3	Flash evaporation 3	Vacuum flash evaporation
COOL-5	Heat Exchanger 5	Preheating of grey water
O_2	Oxidant (O_2)	30.0 °C, 56 bar
STEAM1	Oxidant (Steam)	265.0 °C, 55 bar
COAL	Coal	46.5 °C, 1 bar

- The syngas output from the gasifier only includes H_2, CO, CO_2 and CH_4, and other gas compositions are not considered.
- In this study, the coal used was of a single type, and the influence of the type and grade of coal on the experimental results was not considered.

2.4. Calculation methods

2.4.1. Material balance calculation

According to the law of conservation of mass, the mass of materials entering a specific process should be equal to the total mass of materials leaving the system and the losses at each stage of the process. The expression is as follows:

$$\sum m_{input} = \sum m_{output} + \sum m_{consum} \tag{9}$$

$$\eta = \left(\sum m_r - \sum m_p\right) \Big/ \left(\sum m_r\right) \times 100\% \tag{10}$$

Where m_{input} denotes the amount of material input into the system within a unit of time, kg/h, m_{output} denotes the amount of material output of the system within a unit of time, kg/h, m_{consum} denotes system loss per unit time, kg/h, η represents the loss rate,%, indicating the proportion of material mass lost during the production process to the total consumption. $\sum m_r$ denotes the consumption of a certain raw material, kg/h, $\sum$

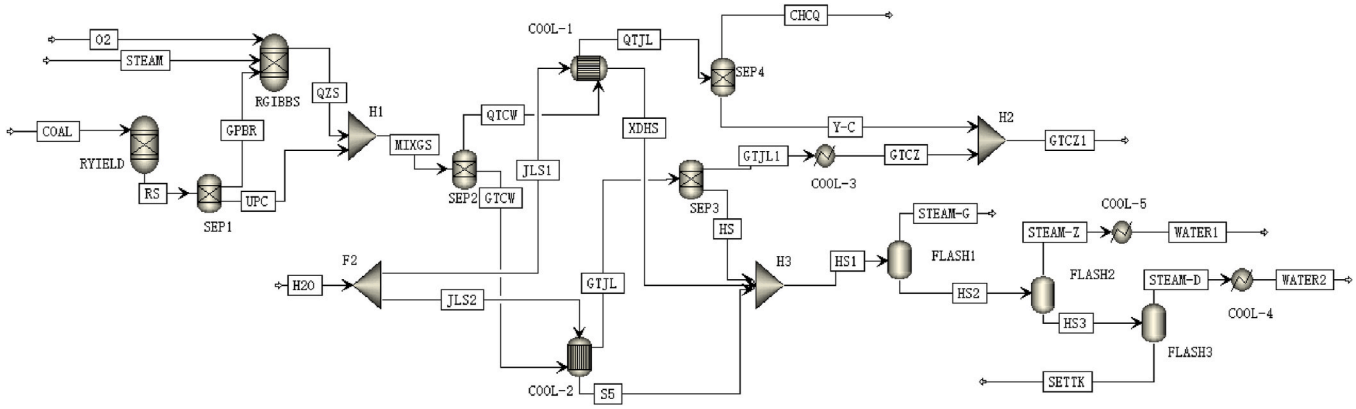

Fig. 2. Simulation model of coal-water slurry gasification process.

m_p denotes the output of a certain product, kg/h.

2.4.2. Exergy analysis

Exergy refers to the work done by a system to the outside world during the reversible process when it reaches equilibrium with the reference state of the environment from any state it is in (with certain temperature, pressure and chemical composition) within a definite system. The environmental reference state refers to an idealized external environment with limited conditions, composed of selected reference material systems within the Earth's scope such as the atmosphere, surface, and ocean, which are in a completely balanced state. It has an environmental reference temperature of 298.15 K and an environmental reference pressure of 100 kPa and serves as the numerical basis for exergy analysis calculations.

When conducting exergy analysis on the system, the exergy equilibrium principle should be followed. The exergy equilibrium equation is as follows:

$$\sum_{K_{in}=1}^{n} E_{K_{in}} + E_Q = \sum_{K_{out}=1}^{m} E_{K_{out}} + \Delta E_f \tag{11}$$

$$E_K = E_w + E_h \tag{12}$$

Where $E_{K_{in}}$ refers to the exergy value of the input logistics, kW, E_Q refers to the heat exergy of the input logistics,kW, $E_{K_{out}}$ refers to the exergy value of the output logistics,kW, ΔE_f refers to the exergy loss of the system,kW, E_K refers to the exergy value of the system,kW, E_w refers to the physical exergy of the system,kW, E_h refers to the chemical exergy of the system, kW. The calculation formulas of E_w and E_h are as follows (GBT1409-2021 Exergy Analysis Technical Guidelines for Energy Systems):

$$E_w = (H - H_0) - T_0(S - S_0) \tag{13}$$

$$E_h = \sum\nolimits_i X_i E_{chi} + \mathrm{R}T_0 \sum\nolimits_i X_i \ ln\ X_i \tag{14}$$

Where H refers to the enthalpy value of the system under a given state (given temperature and pressure), kJ/mol, H_0 refers to the enthalpy value of the system under the environmental reference state (298.15 K, 100 kPa), kJ/mol, S refers to the state entropy value of the system under a given state, kJ/mol, S_0 refers to the state entropy value of the system in the environmental reference state (298.15 K, 100 kPa), kJ/mol, X_i refers to the molar fraction of component i, E_{chi} refers to the standard exergy of component i, kJ/mol, R refers to the ideal gas constant, 8.314 kJ $kmol^{-1}$ K^{-1}, T_0 refers to the ambient reference temperature, K.

Coal is a complex substance without a fixed chemical composition. Its standard exergy can be estimated by the following formula based on its high or low calorific value (GBT1409-2021 Exergy Analysis Technical Guidelines for Energy Systems):

$$E_g^\theta = a_g\left(\Delta_c H_g\right)^2 + b_g \Delta_c H_g + c_g\left(12400 < \Delta_c H_g < 55200\right) \tag{15}$$

$$E_l^\theta = a_l(\Delta_c H_l)^2 + b_l \Delta_c H_l + c_l(5500 < \Delta_c H_l < 48600) \tag{16}$$

Where E_g^θ, E_l^θ, E_s^θ are respectively the estimated values of the standard exergy of gaseous, liquid and solid fuels, kJ/kg, $\Delta_c H_g$, $\Delta_c H_l$, $\Delta_c H_s$ are respectively the high or low calorific values of gaseous, liquid and solid fuels, in kJ/kg, a_g, b_g, c_g, a_l, b_l, c_l, a_s, b_s, c_s are the corresponding coefficients of the high or low calorific value of the fuel respectively. The specific values are shown in Table 2.

3. Results and discussion

3.1. Model validation

Based on the simplified coal-water slurry gasification, the reliability of the constructed model was verified. The coal used in industrial production and the coal input in the model are of the same type. The proximate and ultimate analysis of coal are shown in Table 3. The parameters of the input logistics in the model are shown in Table 1. The simulation results of the model are compared with the actual production data of the factory, and the results are shown in Table 4.

The results show that the simulation results of the model are basically consistent with the actual production data of the factory, and the error is within the allowable range of the project (±5 %), proving the accuracy and reliability of the constructed model.

Table 2
The coefficients of the formula when using high calorific value or low calorific value.

State	Combustion value kJ/kg	a	b	c
Gaseous (g)	High calorific value	-1.2983×10^{-6}	1.05610	-9.4419×10^{2}
	Low calorific value	-2.5351×10^{-6}	1.19150	-1.7133×10^{3}
Liquid (l)	High calorific value	-2.5674×10^{-6}	1.12700	-5.9389×10^{2}
	Low calorific value	-1.8804×10^{-6}	1.13240	-4.9754×10^{2}
Solid (s)	High calorific value	-2.2668×10^{-8}	0.97864	-1.3779×10^{3}
	Low calorific value	-5.6089×10^{-8}	1.00780	-1.9642×10^{3}

3.2. Analysis of material transformation

Studied the material flow situation of the entire process, and through material flow analysis, the raw material conversion path and the process were tracked. Fig. 3 shows the production material flow under a certain oxidant ratio. The total amount of materials input into the system is 101.070 kg/h, among which 94.79 % of the materials are used in the gasification process and 5.21 % of the materials are used to produce high-pressure steam. Among them, for the materials conveyed to the gasification process, 20.87 % of the materials are used to maintain the operation of the equipment, and 79.13 % of the materials are used for the gasification reaction to produce syngas (the proportions of steam, oxygen, and coal-water slurry were 42.22 %, 22.69 %, and 35.09 % respectively). After the raw materials undergo gasification reaction, synthesis gas mainly composed of H_2, CO and CO_2 are generated (accounting for 61.28 % of the total materials), and at the same time, a certain amount of steam (32.04 %), residue (4.07 %) and unreacted residual carbon (2.38 %) are produced. After calculation, the material loss rate of this process is 6.56 % and the carbon conversion rate is 97.62 %. Furthermore, the molar composition of the Crude synthesis gas includes 39.92 % H_2, 41.24 % CO, 17.97 % CO_2 and 0.87 % CH_4.

3.3. Analysis of energy-saving potential

The energy system follows the law of conservation. The total energy input to the system is equal to the sum of the output energy and energy consumption. In industrial production, the level of energy consumption is an important indicator for evaluating equipment performance, process characteristics, operating conditions and economy. The gasification process, as a system, takes in energy mainly from coal, O_2, steam and electricity. The energy contained in the generated crude syngas

Table 3
Proximate and ultimate analysis of coal.

Proximate analysis (wt.%)				Ultimate analysis (wt.%)				
M_{ad}	FC_{ad}	V_{ad}	A_{ad}	C_{ad}	H_{ad}	N_{ad}	S_{ad}	O_{ad}
8.00	53.83	35.00	11.17	65.30	5.06	0.60	0.34	17.53

Table 4
Comparison of model simulation values with factory production data.

Project	Volume fractions of component in the synthesis gas/%			
	H_2	CO	CO_2	CH_4
Model simulation value	39.908	41.168	18.921	0.003
Factory production data	39.900	41.170	18.925	0.005
Error/%	0.8	−0.2	−0.4	−0.2

represents the effective energy that the system can output. The gasification unit is an important unit of this process. The transformation of substances and energy is mainly accomplished through unit reactions. Firstly, the influence of O_2 and steam input on the energy consumption of the equipment was studied, and the results are shown in Fig. 4. The energy flow among each unit of the process and the exergy loss distribution of the system are shown in Figs. 5 and 6.

3.3.1. *Comprehensive effect of O_2 and steam input on the energy consumption of the equipment*

Fig. 4 shows that increasing the steam input leads to an increase in equipment energy consumption, while increasing the O_2 input reduces the equipment energy consumption. During the reaction process, steam mainly participates in the water-gas reaction and the water-gas shift reaction, namely reactions (3) and (6). Increasing the steam input will intensify the endothermic reaction, consume more system energy and cause the system temperature to decrease. To maintain the temperature required for the reaction, more energy needs to be supplemented additionally, resulting in an increase in energy consumption. The increase in O_2 input promotes combustion reactions, releases a large amount of heat, and reduces the demand for external heating. Meanwhile, the temperature inside the furnace has been increased, the reaction rate has been promoted, and the energy consumption of the equipment has been reduced. In the actual operation process, energy consumption can be reduced by reasonably regulating the ratio of steam to O_2.

3.3.2. *Energy flow and exergy loss analysis*

Fig. 5 indicates that exergy loss exists in each unit of the system. The exergy loss of the gasification unit is mainly caused by the incomplete conversion of carbon (due to the influence of process characteristics, some carbon does not participate in the reaction and directly flows to the subsequent units in the form of residual carbon) and the change of thermal energy grade between different reactions. The exergy loss of the

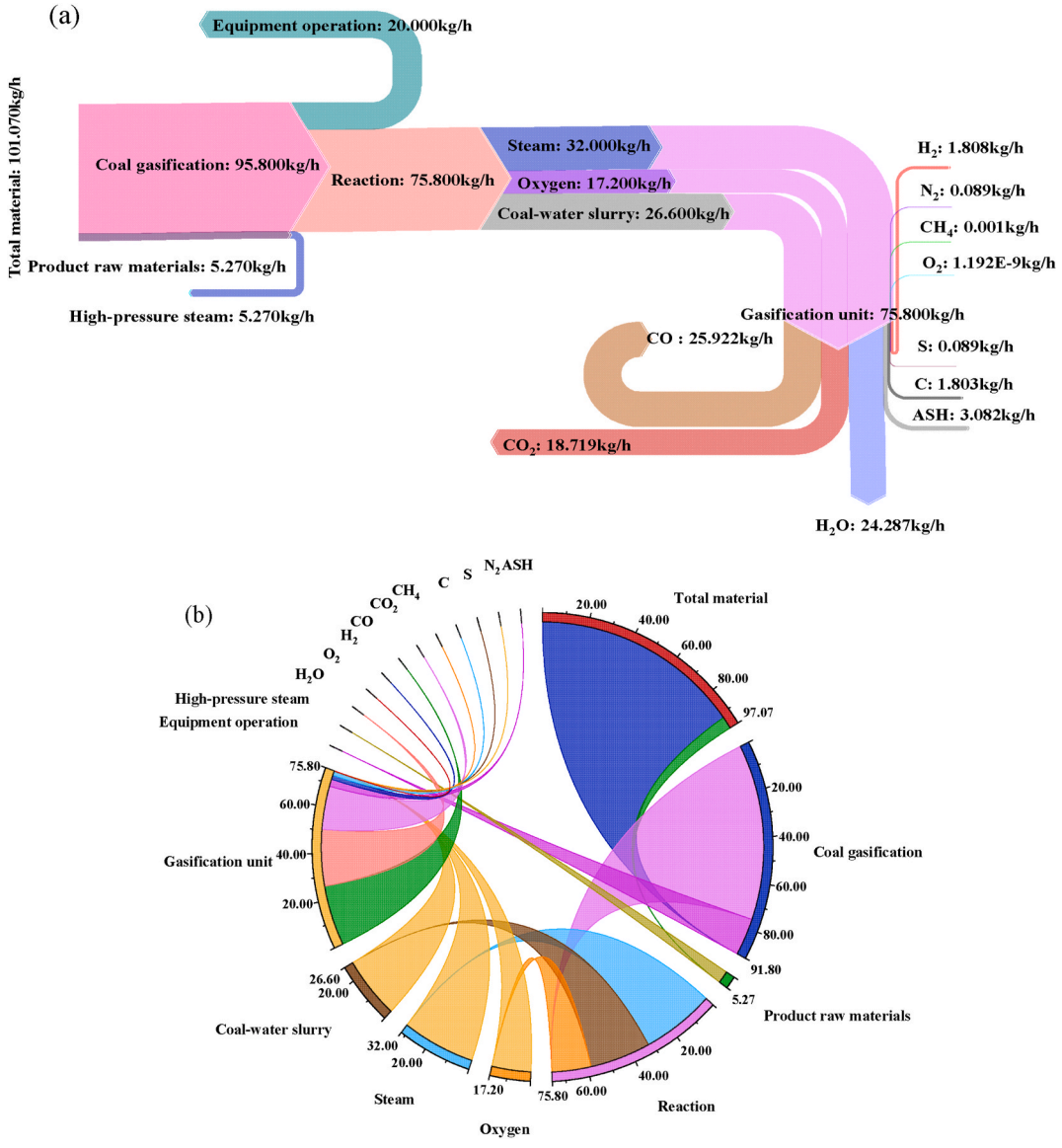

Fig. 3. Material flow of production (a) and material distribution (b) under a certain oxidant ratio.

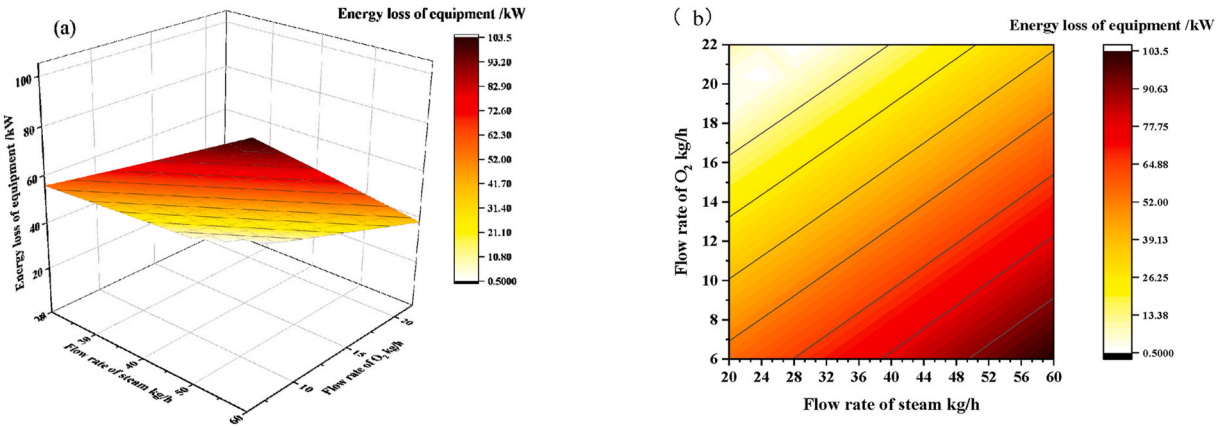

Fig. 4. The influence of O_2 and steam input on energy consumption, 3D (a) and 2D (b).

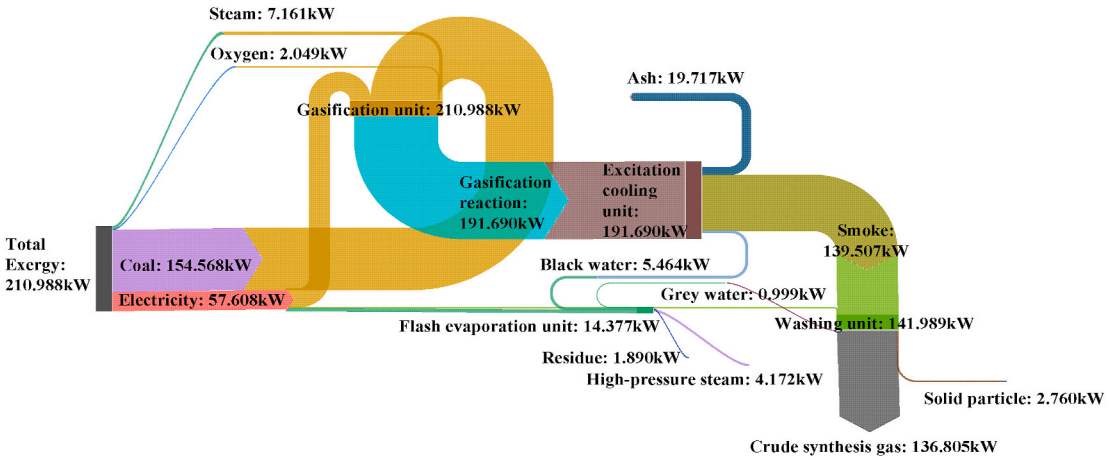

Fig. 5. Process of energy flow.

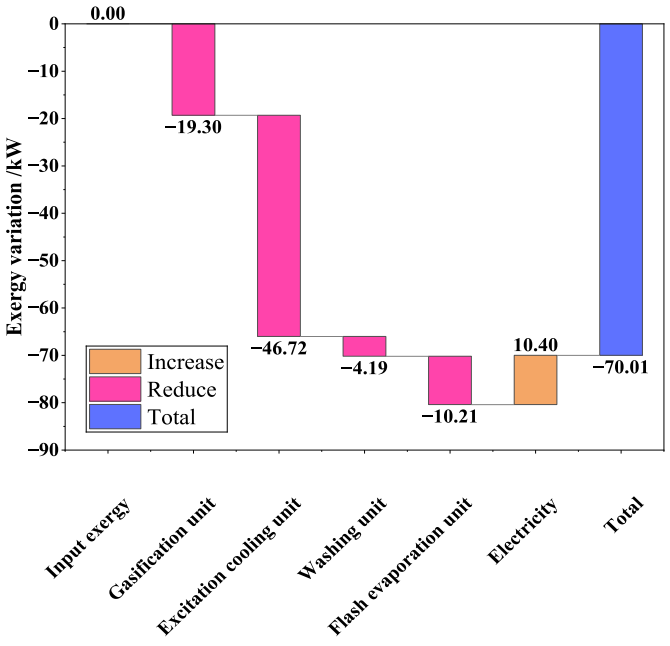

Fig. 6. Exergy loss of the system.

excitation cooling unit is mainly caused by the direct cooling of the syngas by water. The sensible heat of the high-temperature syngas evaporates the liquid water, and the original high-grade thermal energy is converted into low-grade steam thermal energy, resulting in significant exergy loss. The washing unit completes the washing of crude syngas, and impurity gases and solid particles are separated. During the process, additional electrical energy is required to maintain the operation of the equipment, and the total energy of the unit remains basically unchanged. The flash evaporation unit also requires additional electrical energy to maintain the operation of the equipment. Compared with the front washing unit, the total exergy of this unit increases. After the flash is completed, the total exergy value decreases.

Fig. 6 shows that the total exergy loss of the entire process reaches 70.01 kW, accounting for 33.18 % of the total exergy of the system. The exergy loss of the system mainly occurs in the excitation cooling unit, reaching 46.72 kW, accounting for 66.73 % of the total exergy loss of the system. Secondly, the gasification unit has an exergy loss of 19.30 kW, accounting for 27.57 % of the total exergy loss of the system. The exergy loss of the washing unit reached 4.18 kW, accounting for 5.97 % of the total exergy loss of the system. The exergy loss of the flash evaporation unit reached 10.21 kW, accounting for 14.58 % of the total exergy loss of the system.

3.3.3. *Energy conservation analysis*

Based on the above analysis results, this process has huge energy-saving potential, mainly focusing on the excitation cooling unit, gasification unit and flash evaporation unit (contributing 66.73 %, 27.57 % and 14.58 % of exergy losses respectively).

For the optimization of the excitation cooling unit, a radiant waste pot can be adopted to replace the traditional rapid cooling process, and the water-cooled wall can absorb part of the radiant heat of the high-temperature gas. The water in the water-cooled wall is heated and rises to the steam drum. The high-pressure steam generated by the steam drum can be sent to the steam network. This enables heat recovery and reduces exergy loss.

For the energy-saving optimization of the gasification unit, an advanced control system can be adopted to achieve the dynamic regulation of the oxygen, steam-coal ratio and reduce the irreversible heat loss of the reaction. Meanwhile, the introduction of a reaction catalyst can be considered to lower the gasification reaction temperature and increase the reaction rate, thereby reducing the overall energy consumption [41].

The energy loss existing in the flash evaporation unit can be recovered as waste heat through direct heat exchangers or Organic Rankine Cycles (ORC), etc., and be used for industrial heating and power generation [42]. In the three-stage flash evaporation of black water, the high-pressure steam generated at each stage can be used in steam pipelines and for preheating grey water, etc.

3.4. Analysis of carbon reduction potential

Coal-water slurry usually has a relatively high-water content (30–40 %), and due to the use of steam as the gasification agent, the gasification reaction products contain a large amount of CO_2. In addition, maintaining the operation of each equipment also indirectly promotes the emission of CO_2. Firstly, studying the influence of raw material ratio on the yield of CO_2 and the effective conversion rate of carbon (CO). Taking the input amounts of O_2 and steam as variables, the sensitivity analysis was conducted, and the results are shown in Figs. 7 and 8. In addition, the CO_2 emissions among each unit of the process were studied, including the CO_2 emissions caused by the operation of the equipment. The results are shown on Fig. 9.

3.4.1. Comprehensive effect of O_2 and steam input on the yields of CO and CO_2

Fig. 7 indicates that an increase in the input of O_2 and steam will both lead to an increase in the yield of CO_2, and vice versa. The influence of laws of the two variables on the yield of CO is opposite to this. Increasing the flow rate of O_2 promotes the forward progress of reaction (2), and increasing the flow rate of steam promotes the forward progress of reaction (6), both of which lead to an increase in the yield of CO_2. The results in Fig. 8 verify this view. As reaction (6) proceeds forward, a large amount of CO is consumed, the yield of CO decreases, and the flow rate of O_2 increases, making reaction (2) dominant and reaction (1) restricted, resulting in a decrease in the yield of CO.

3.4.2. Analysis of carbon footprint flow

Fig. 9 shows the carbon footprint flow of the entire process. The results show that among the raw coal, 38.56 % of the coal is used to provide electricity. Among them, 52.35 % of the electrical energy is used to maintain the operation of the flash evaporation unit, 47.60 % of the electrical energy is used to maintain the operation of the gasification unit, and the remaining electrical energy is used to maintain the operation of the washing unit. Furthermore, 51.28 % of the raw coal enters the gasification system to participate in the reaction, and after being transformed into smoke and ASH (in actual cases, some are retained in water as tar and phenolic substances), it flows into the subsequent treatment unit. 10.16 % of the raw coal is used to produce high-pressure steam. After the smoke was washed, crude synthesis gas and residual carbon were separated. In the separate crude synthesis gas, carbon mainly existed in the form of CO_2 and CO, with mass fraction rates of 41.93 % and 58.07 % respectively. The CO_2 emission rate shows that the gasification unit is the main source of CO_2 emissions, contributing to 74.98 % of the CO_2 in the entire system. Next are the flash evaporation unit and the washing unit, contributing 20.62 % and 4.4 % of the CO_2 in the entire system respectively.

3.4.3. Analysis of carbon reduction

Based on the above analysis results, the carbon emissions of the system can be reduced by adjusting the ratio of raw materials (oxygen and steam flow rates), introducing reaction catalysts and optimizing the flash evaporation system. Reducing the input of steam and oxygen can limit the water-gas shift reaction and combustion reaction, and it is estimated to reduce CO_2 emissions by 5.5–12.4 %. Introducing a reaction catalyst can increase the reaction rate, shorten the reaction time, enhance the carbon conversion rate, promote the concentrated generation of CO_2, and be more conducive to the capture and storage of CO_2 [43]. Meanwhile, it is also necessary to balance the energy consumption of the equipment to avoid an increase in CO_2 emissions caused by high energy consumption of the equipment. Optimize the flash evaporation system, adopt multi-stage flash evaporation, improve the utilization rate of waste heat, reduce energy consumption, and indirectly lower carbon emissions.

4. Conclusion

Constructed the model of coal-water slurry gasification with the help of Aspen Plus. Combined with the analytical method of coupling MFA and Exergy analysis, we explored the energy-saving and carbon reduction potential of this process and put forward corresponding optimization suggestions. The main conclusions are as follows.

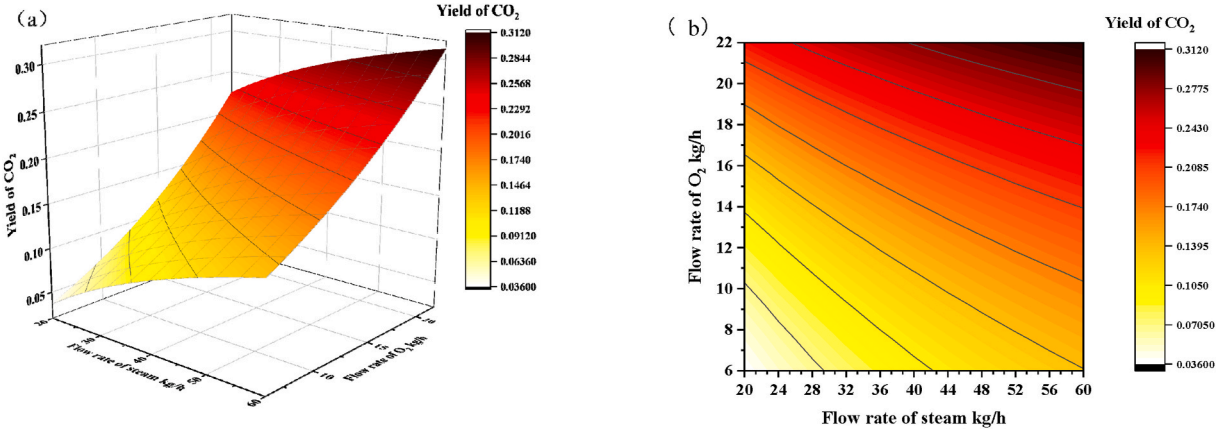

Fig. 7. The influence of O_2 and steam input on the yield of CO_2, 3D (a) and 2D (b).

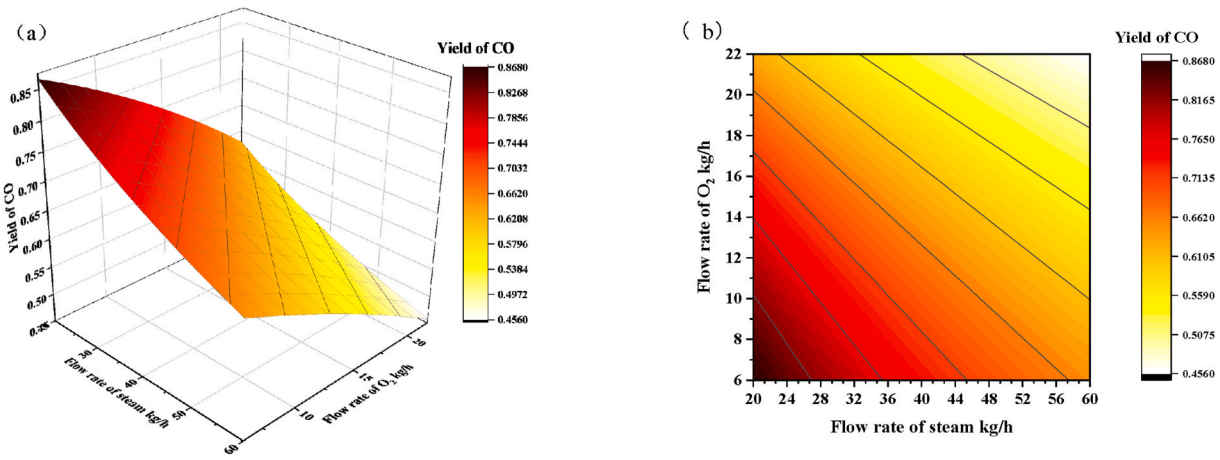

Fig. 8. The influence of O_2 and steam input on the yield of CO, 3D (a) and 2D (b).

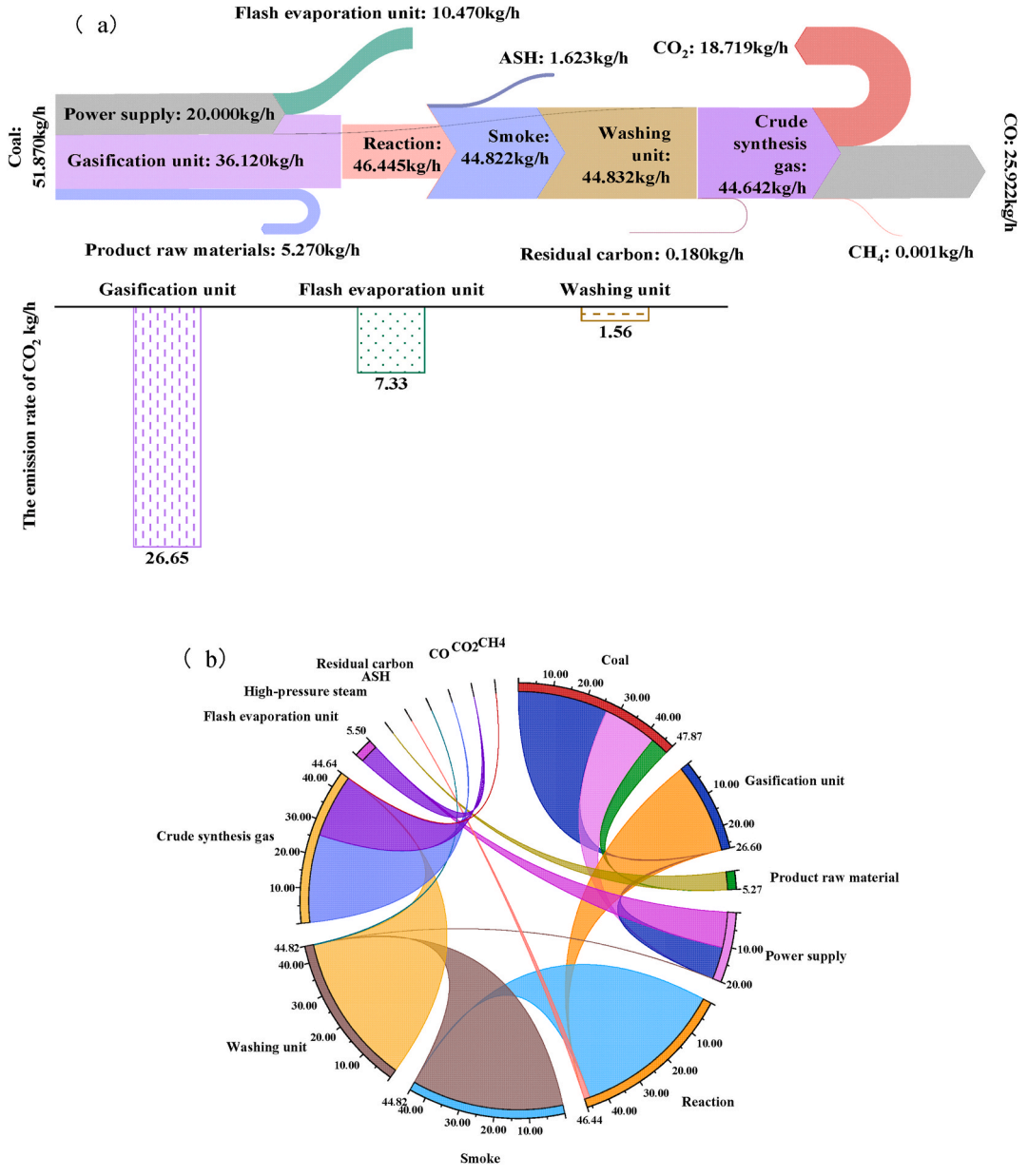

Fig. 9. The carbon footprint flow (a) and carbon emission distribution (b) of the production process.

(1) After the gasification reaction of steam, oxygen and coal-water slurry, crude synthesis gas (accounting for 61.28 % of the total materials), steam (32.04 %), residue (4.07 %) and unreacted carbon residue (2.38 %) are produced. After calculation, the material loss rate of this process is 6.56 % and the carbon conversion rate is 97.62 %. The molar composition of the crude syngas is 39.92 % H_2, 41.24 % CO, 17.97 % CO_2 and 0.87 % CH_4.
(2) Reducing the steam input and increasing the oxygen input can help lower the energy consumption of the equipment. The total exergy loss of the system accounts for 33.18 % of the total exergy of the system. Among them, the exergy loss mainly occurs in the excitation cooling unit, accounting for 66.73 % of the total exergy loss of the system. Secondly, there are the gasification unit, flash evaporation unit and washing unit, with exergy losses of 27.57 %, 14.58 % and 5.97 % respectively. It is suggested to adopt the radiation waste pot instead of the traditional rapid cooling process and adopt methods such as direct heat exchangers or Organic Rankine Cycles (ORC) to reduce the exergy loss per unit.
(3) Raw coal provides public facilities for the production process, participates in reactions and the production of high-pressure steam. The carbon footprint shows that most of the carbon involved in the reaction eventually exists in the form of CO_2 and CO, which are sent downstream for treatment as the effective components of the crude syngas. The carbon emissions of the entire system are concentrated in the gasification unit, flash evaporation unit and washing unit, and the emission rates of CO_2 are 74.98 %, 20.62 % and 4.40 % respectively. Carbon emissions can be reduced to varying degrees by decreasing the input of oxygen and steam, introducing reaction catalysts and optimizing the flash evaporation system.

This research enriches the theoretical achievements of coal-water slurry gasification, which is conducive to achieving energy conservation and carbon reduction of this technology and is beneficial to the clean and efficient production of syngas. In the long run, it is of great significance to respond to the increasingly severe energy security crisis.

CRediT authorship contribution statement

Chao Linghu: Writing – review & editing, Writing – original draft, Resources, Methodology, Investigation, Formal analysis, Data curation, Conceptualization. **Binxuan Zhou:** Writing – review & editing, Supervision, Project administration, Funding acquisition, Conceptualization. **Xingxing Cheng:** Writing – review & editing, Supervision, Project administration, Funding acquisition. **Jiansheng Zhang:** Resources, Investigation. **Wenlong Mo:** Investigation, Funding acquisition.

Data availability

Data will be made available on request.

Declaration of competing interest

The authors declare that they have no known competing financial interests or personal relationships that could have appeared to influence the work reported in this paper.

Acknowledgements

The author thanks the Key Research and Development Program of Shanxi Province (NO. 202201090301002) and the Strategic Research Project of Shanxi Research Institute of Huairou Laboratory (NO. 2023SY1001) for their support of this work.

References

[1] Chen S, Nouseen S. Tackling economic policy uncertainty and improving energy security through clean energy change. Energy 2025;315:134356. https://doi.org/10.1016/j.energy.2024.134356.
[2] Hille E, Angerpointner C. Did geopolitical risks in supplier countries of fossil fuels lead to reduced domestic energy consumption? Evidence from europe. Energy Policy 2025;198:114499. https://doi.org/10.1016/j.enpol.2025.114499.
[3] Xu T, Feng C, Guluzada E, Chao C. Evaluating the advancement of sustainable development objectives in recently industrialized nations by tying gold prices, fossil fuel prices, and energy use. Energy Strategy Rev 2024;56:101575. https://doi.org/10.1016/j.esr.2024.101575.
[4] Zhou X, Xie F, Li H, Zheng C, Zhao X. Understanding inter-term fossil energy consumption pathways in China based on sustainable development goals. Geosci Front 2024;15:101687. https://doi.org/10.1016/j.gsf.2023.101687.
[5] Solaymani S. Energy security and its determinants in new zealand. Environ Sci Pollut Res 2024;31:51521–39. https://doi.org/10.1007/s11356-024-34611-0.
[6] Aslan A, Ilhan O, Usama A-M, Savranlar B, Polat MA, Metawa N, et al. Effect of economic policy uncertainty on CO_2 with the discrimination of renewable and non renewable energy consumption. Energy 2024;291:130382. https://doi.org/10.1016/j.energy.2024.130382.
[7] Loredana C, Rehman A, Maria Mirabela FI, Pinzon S, Cismaş LM. What implications do primary energy use, urban population agglomeration, and economic development rendered to Romania's environmental sustainability? Energy Strategy Rev 2024;53:101399. https://doi.org/10.1016/j.esr.2024.101399.
[8] Wang K, Wei Y-M. China's regional industrial energy efficiency and carbon emissions abatement costs. Appl Energy 2014;130:617–31. https://doi.org/10.1016/j.apenergy.2014.03.010.
[9] Chen J, Zhang J. The nexus between green finance and energy consumption in regional comprehensive economic partnership countries. Environ Sci Pollut Res 2024;31:14071–87. https://doi.org/10.1007/s11356-024-32003-y.
[10] Bashir MF, Bashir MA, Raza SA, Bilan Y, Vasa L. Linking gold prices, fossil fuel costs and energy consumption to assess progress towards sustainable development goals in newly industrialized countries. Geosci Front 2024;15:101755. https://doi.org/10.1016/j.gsf.2023.101755.
[11] Rahman A, Murad SMW, Mohsin AKM, Wang X. Does renewable energy proactively contribute to mitigating carbon emissions in major fossil fuels consuming countries? J Clean Prod 2024;452:142113. https://doi.org/10.1016/j.jclepro.2024.142113.
[12] Liu M, Ma B. China's electricity conversion strategy in energy statistics: impacts on key energy metrics and induced incentive distortions in low-carbon transition. Energy Sustain Dev 2024;80:101458. https://doi.org/10.1016/j.esd.2024.101458.
[13] Sahu SG, Chakraborty N, Sarkar P. Coal-biomass co-combustion: an overview. Renew Sustain Energy Rev 2014;39:575–86. https://doi.org/10.1016/j.rser.2014.07.106.
[14] Ueki Y, Yoshiie R, Naruse I. Combustion behavior of pulverized coal and ash particle properties during combustion. ISIJ Int 2015;55:1305–12. https://doi.org/10.2355/isijinternational.55.1305.
[15] Kamble AD, Saxena VK, Chavan PD, Mendhe VA. Co-gasification of coal and biomass an emerging clean energy technology: status and prospects of development in Indian context. Int J Min Sci Technol 2019;29:171–86. https://doi.org/10.1016/j.ijmst.2018.03.011.
[16] Kato K, Matsueda K. Leading edge of coal utilization technologies for gasification and cokemaking. KONA Powder Part J 2018;35:112–21. https://doi.org/10.14356/kona.2018018.
[17] Chen J, Wang Q, Xu Z, E J, Leng E, Zhang F, et al. Process in supercritical water gasification of coal: a review of fundamentals, mechanisms, catalysts and element transformation. Energy Convers Manag 2021;237:114122. https://doi.org/10.1016/j.enconman.2021.114122.
[18] Cao Y, He B, Ding G, Su L, Duan Z. Energy and exergy investigation on two improved IGCC power plants with different CO_2 capture schemes. Energy 2017;140:47–57. https://doi.org/10.1016/j.energy.2017.08.044.
[19] Ptasinski KJ, Prins MJ, Pierik A. Exergetic evaluation of biomass gasification. Energy 2007;32:568–74. https://doi.org/10.1016/j.energy.2006.06.024.
[20] Wang F, Yu G, Liu H, Li W, Guo Q, Xu J, et al. Opposed multi-burner gasification technology: recent process of fundamental research and industrial application. Chin J Chem Eng 2021;35:124–42. https://doi.org/10.1016/j.cjche.2021.07.007.
[21] Smolinski A, Wochna S, Howaniec N. Gasification of lignite from polish coal mine to hydrogen-rich gas. Int J Coal Sci Technol 2022;9:77. https://doi.org/10.1007/s40789-022-00550-9.
[22] Jiang B, Raza MY. Research on China's renewable energy policies under the dual carbon goals: a political discourse analysis. Energy Strategy Rev 2023;48:101118. https://doi.org/10.1016/j.esr.2023.101118.
[23] Tan X, Lai H, Gu B, Zeng Y, Li H. Carbon emission and abatement potential outlook in China's building sector through 2050. Energy Policy 2018;118:429–39. https://doi.org/10.1016/j.enpol.2018.03.072.
[24] Kappagantula RV, Ingram GD, Vuthaluru HB. Effectiveness of three reactor chemical looping for ammonia production using aspen plus simulation. Int J Hydrogen Energy 2024;61:1340–55. https://doi.org/10.1016/j.ijhydene.2024.02.238.
[25] Patcharavorachot Y, Pradiskhean S, Aentung T, Saebea D, Arpornwichanop A. Co-pyrolysis of biomass/polyurethane foam waste: thermodynamic study using Aspen Plus. J Anal Appl Pyrolysis 2024;183:106833. https://doi.org/10.1016/j.jaap.2024.106833.
[26] Qi J, Liu J, Chen G, Yao J, Yan B, Yi W, et al. Hydrogen production from municipal solid waste via chemical looping gasification using $CuFe_2O_4$ spinel as oxygen

carrier: an Aspen Plus modeling. Energy Convers Manag 2023;294:117562. https://doi.org/10.1016/j.enconman.2023.117562.
[27] Wan H, Feng F, Yan B, Liu J, Chen G, Yao J. Methanation of syngas from biomass gasification in a dual fluidized bed: an Aspen plus modeling. Energy Convers Manag 2024;318:118902. https://doi.org/10.1016/j.enconman.2024.118902.
[28] Zhou B, Chang J, Li J, Hong J, Wang T, Zhu Z, et al. Two-stage gasification process simulation and optimization of pulverized coal for hydrogen-rich production using Aspen plus. Int J Hydrogen Energy 2024;49:849–60. https://doi.org/10.1016/j.ijhydene.2023.08.033.
[29] Salisu J, Gao N, Quan C, Yanik J, Artioli N. Co-gasification of rice husk and plastic in the presence of CaO using a novel ANN model-incorporated Aspen plus simulation. J Energy Inst 2023;108:101239. https://doi.org/10.1016/j.joei.2023.101239.
[30] Gündüz Han D, Erdem K, Midilli A. Investigation of hydrogen production via waste plastic gasification in a fluidized bed reactor using Aspen Plus. Int J Hydrogen Energy 2023;48:39315–29. https://doi.org/10.1016/j.ijhydene.2023.07.038.
[31] Wu F-H, Hsu Y-T. Parameter study of waste shiitake substrate/waste polyethylene Co-gasification using Aspen Plus kinetic modeling. Int J Hydrogen Energy 2024;83:29–38. https://doi.org/10.1016/j.ijhydene.2024.08.089.
[32] Zhao Y, Yao J, Chen G, Liu J, Cheng Z, Wang L, et al. Energy, efficiency, and environmental analysis of hydrogen generation via plasma co-gasification of biomass and plastics based on parameter simulation using Aspen plus. Energy Convers Manag 2023;295:117623. https://doi.org/10.1016/j.enconman.2023.117623.
[33] Alobaid F, Almohammed N, Massoudi Farid M, May J, Rößger P, Richter A, et al. Progress in CFD simulations of fluidized beds for chemical and energy process engineering. Prog Energy Combust Sci 2022;91:100930. https://doi.org/10.1016/j.pecs.2021.100930.
[34] Tang Z, Sui M, Wang X, Xue W, Yang Y, Wang Z, et al. Theory-guided deep neural network for boiler 3-D NOx concentration distribution prediction. Energy 2024;299:131500. https://doi.org/10.1016/j.energy.2024.131500.
[35] Naqvi SR, Hameed Z, Tariq R, Taqvi SA, Ali I, Niazi MBK, et al. Synergistic effect on co-pyrolysis of rice husk and sewage sludge by thermal behavior, kinetics, thermodynamic parameters and artificial neural network. Waste Manag 2019;85:131–40. https://doi.org/10.1016/j.wasman.2018.12.031.
[36] Masoud Parsa S, Yazdani A, Aberoumand H, Farhadi Y, Ansari A, Aberoumand S, et al. A critical analysis on the energy and exergy performance of photovoltaic/thermal (PV/T) system: the role of nanofluids stability and synthesizing method. Sustain Energy Technol Assessments 2022;51:101887. https://doi.org/10.1016/j.seta.2021.101887.
[37] Tirupati Rao V, Raja Sekhar Y, Arıcı M, Ralph Pochont N, Reddy Prasad DM. Experimental investigations on bi-symmetrical web flow water based photovoltaic-thermal (PVT) system: energy, exergy, and entropy (3-E) analysis. Sol Energy 2024;271:112445. https://doi.org/10.1016/j.solener.2024.112445.
[38] Sun W, Wang Q, Zhou Y, Wu J. Material and energy flows of the iron and steel industry: status quo, challenges and perspectives. Appl Energy 2020;268:114946. https://doi.org/10.1016/j.apenergy.2020.114946.
[39] Burmistrz P, Chmielniak T, Czepirski L, Gazda-Grzywacz M. Carbon footprint of the hydrogen production process utilizing subbituminous coal and lignite gasification. J Clean Prod 2016;139:858–65. https://doi.org/10.1016/j.jclepro.2016.08.112.
[40] Zhang S, Lv L, Liu L, Dai F, Sui J. An efficient low-carbon hydrogen production system based on novel staged gasification coupling with chemical looping technology. Energy Convers Manag 2025;328:119625. https://doi.org/10.1016/j.enconman.2025.119625.
[41] Yu J, Guo Q, Gong Y, Ding L, Wang J, Yu G. A review of the effects of alkali and alkaline earth metal species on biomass gasification. Fuel Process Technol 2021;214:106723. https://doi.org/10.1016/j.fuproc.2021.106723.
[42] Mahmoudi A, Fazli M, Morad MR. A recent review of waste heat recovery by organic rankine cycle. Appl Therm Eng 2018;143:660–75. https://doi.org/10.1016/j.applthermaleng.2018.07.136.
[43] Song Q, Zhao H, Ma Q, Yang L, Ma L, Wu Y, et al. Catalytic upgrading of coal volatiles with Fe_2O_3 and hematite by TG-FTIR and py-GC/MS. Fuel 2022;313:122667. https://doi.org/10.1016/j.fuel.2021.122667.